PROBLEMY KOLEJNICTWA
RAILWAY REPORT
Issue 186 (March 2020)
DOI: 10.36137/1866E
ISSN 0552-2145 (print) ISSN 2544-9451 (on-line)

Analysis of the Ways to Identify Rail Running Surface Defects by Means of Vibration Signals

Roksana LICOW[1], Franciszek TOMASZEWSKI[2]

Summary
The article discusses a preliminary concept of a method enabling the identification of chosen rail running surface defects, such as squats, spalling, and running surface defects, by analysing the parameters of vibration signals. It features a description of the methodology of the conducted tests, the scope thereof, and the selection of the measurement points with specific defect types. The article covers selected results of vibration tests, the results of analyses of recorded signals for defective track sections and those for control track sections. The presented measurement results have been obtained for the technical–operating conditions occurring on railway line no. 213 Reda – Hel and line no. 131 Chorzów Batory – Tczew. The preliminary test results and conclusions included in the article show that it is reasonable to pursue further research into the phenomena involving the utilisation of vibroacoustics in rail performance diagnostics.

Keywords: vibroacoustics, squat, spalling, running surface defect

1. Introduction

The article describes a concept of how to use vibroacoustic signals to determine the condition of the rail running surface and discusses an analysis of the possible ways to identify the occurring defects [6]. The tests were conducted on two railway lines – no. 213 Reda – Hel and no. 131 Chorzów Batory – Tczew at eight measurement points, analysing the three most common defects of rail running surface.

The analysis of vibration signals was performed on the following running surface defects: squat (defect no. 227), spalling (defects 2251, 2252), and defect no. 221 – running surface defect.

The first defect subject to analysis was defect no. 227 in accordance with PLK's Catalogue of Rail Defects. A squat defect is defined as a crack and local indentation of a rail's running surface, occurring outside rail ends on the running surface of a railhead, on straight sections of a track and on elevations of a grade of up to 4.0‰ (Fig. 1) [3].

At its earliest stage, a squat appears to be a dark semicircular spot, often still without any cracks. Further stages of its development involve material peeling off and cracking. The lack of appropriate diagnostics of rails as well as no visual inspections and no application of proper preventive measures may lead to rails breaking completely and trains derailing. The causes of this type of defect are not fully known, hence it is important to perform appropriate diagnostics involving, among others, careful visual inspections of the occurring defects and rail observations involving ultrasound testing [4, 6].

Fig. 1. Squat defect on railway line no. 213 Reda – Hel [authors' own work]

[1] Ph.D. Eng.; Gdańsk University of Technology, Faculty of Civil and Environmental Engineering; e-mail: roksana.licow@pg.edu.pl.
[2] Prof. Ph.D. Eng.; Poznań University of Technology, Faculty of Transport Engineering, Institute of Combustion Engines and Transport; Franciszek.tomaszewski@put.poznan.pl.

The next defect is spalling, defect no. 2252 and no. 2251, single and multiple spalling in accordance with PLK's Catalogue of Rail Defects (Fig. 2). Spalling involves the damage of rail running surfaces resulting entirely from the standard use and operation of rails, found commonly on track sections where trains brake violently or where heavy freight trains are accelerated to operational speed. Spalling occurs most often before home signals as well as before level crossings and turnouts.

Spalling occurs symmetrically on both isolated rail sections and is identified by means of visual inspection. Recommended measures to be taken are observation, grinding, replacement or immediate replacement of the rail [3, 7].

Fig. 2. Spalling defect on railway line no. 213 Reda – Hel [authors' own work]

The last of the analysed defects is the rail running surface defect no. 221 in accordance with PLK's Catalogue of Rail Defects (Fig. 3). Defect no. 221 appears only on the railhead during the standard use and operation of the track. It is damage with a metallurgical origin. Its most common manifestations include shelling of the running surface or groove-shaped cracks.

Fig. 3. Defect 221 – damage of the running surface on railway line no. 213 Reda – Hel [authors' own work]

Damage 221 is identified most often by means of visual inspection. Depending on the degree of defect development, the recommendation is to inspect the rail visually on a continual basis, grind it or re-surface it [3].

The ability to identify a defect and determine the degree of deterioration, as well as the steps to be taken, depends very often on the diagnostic technician's experience and on the conditions in which rail diagnostics is performed. Taking advantage of vibration signals could make the evaluation of the condition of running surfaces and of particular elements of the track superstructure quicker, more effective and more accurate. Using vibroacoustic phenomena acting as a dynamic response of rails during train passage can let us evaluate the condition of the rail running surface, joints, fastenings, sleepers, and railroad ballast [1, 2].

2. Test methodology

2.1. The scope of tests and the location of measurement points

The tests were carried out on two railway lines managed by PKP PLK S.A., on the premises of the Railway Track Development and Construction Unit in Gdynia [PL: Zakład Gdynia]. Railway line no. 213 is the first of the analysed lines. It is found in the Pomeranian Voivodeship and connects the Reda station with the Hel station. It is a regional line, non-electrified and redeveloped in the period 2011–2015. Railway line no. 213 measures 62.827 km in length.

The second analysed line is railway line no. 131 – a line with the highest volume of freight traffic in Poland, formerly referred to as the coal trunk-line. Line no. 131 connects the Chorzów Batory and Tczew stations. Line no. 131 measures 493.391 km in length, and its annual traffic intensity amounts to approximately 30 Tg.

The measurements were performed at eight measurement points for the two above-mentioned railway lines. There were at least nine measurements of vibration for different train types taken at each point. The scope of the tests, including the location, the chainage, and the superstructure type, is specified in Table 1.

The tests were carried out on line no. 213 Reda – Hel at four measurement points: a control track section and a track section with a squat defect, spalling, and a running surface defect. The tests were also carried out at four measurement points on line 131 Chorzów Batory – Tczew: a control track section and a track section with a squat defect, spalling, and a running surface defect [5].

2.2. Vibration measurement methodology

Vibration measurements were taken using two converters: a 4504A type three-axis vibration converter and a 4513-B-001 single-axis vibration converter. The three-axis converter was fitted to the rail web, and the single-axis converter was mounted underneath the rail

Table 1

Vibration measurement points on railway lines no. 213 and no. 131 [8]

Measurement point name	Measurement date	Number of measurements	Investigated defect / / damage	Track superstructure
213 – Control KM 30.900 LT	24.06.2017	10	control track section	S49 type rail, SB-3 fastening, PS-93, sleepers
213 – 227 squat KM 38.760 LT	26. 06.2017	10	squat	
213 – 2252 Spalling KM 11.500 LT	27.06.2017	10	spalling	
213 – 221 Running surface defect KM 16.100 RT	1.07.2017	9	running surface defect	
Measurement point name	**Measurement date**	**Number of measurements**	**Investigated defect / / damage**	**Track superstructure**
131 – Control KM 458.900 RT	9.07.2017	14	control track section	60E1 type rail (2010), fastening SB-3, PS-93 sleepers
131 – 227 squat KM 466.150 LT	10.07.2017	11	squat	
131 – 2252 Spalling KM 458.750 RT	11.07.2017	12	spalling	
131 – 221 Running surface defect KM 458.880 RT	13.07.2017	10	running surface defect	

[Authors' own work]

foot (Fig. 4). The transducers were located directly in the axis of the research defect. The three-axis converter recorded signals in three directions: X – in line with the train movement, Y – transversely to the train movement, Z – perpendicularly to the train movement.

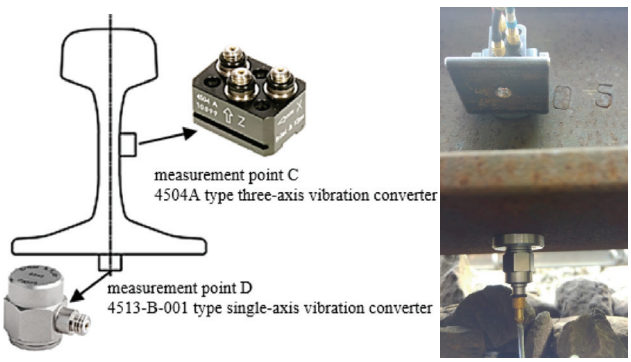

Fig. 4. Placement of vibration measurement converters [authors' own work based on http://www.bruel.com.pl/]

The analysis of the results of the conducted vibration signal tests has been based on the assumption that all wheels of the considered rolling stock are characterised by the same kind and degree of wear.

3. Measurement result analysis

Figures 5–10 show a compilation of measurement results of the RMS values of vibration acceleration for selected running surface defects, including measurements of vibration for control track sections. The curves represent the values over time for the average values of vibration for all measurement samples during train travel.

Figure 5 presents a comparison of the RMS values of vibration acceleration for the control track section with a track section featuring a squat defect on lines no. 213 and no. 131. The results were recorded by a 4513-B-001 single-axis sensor placed under the

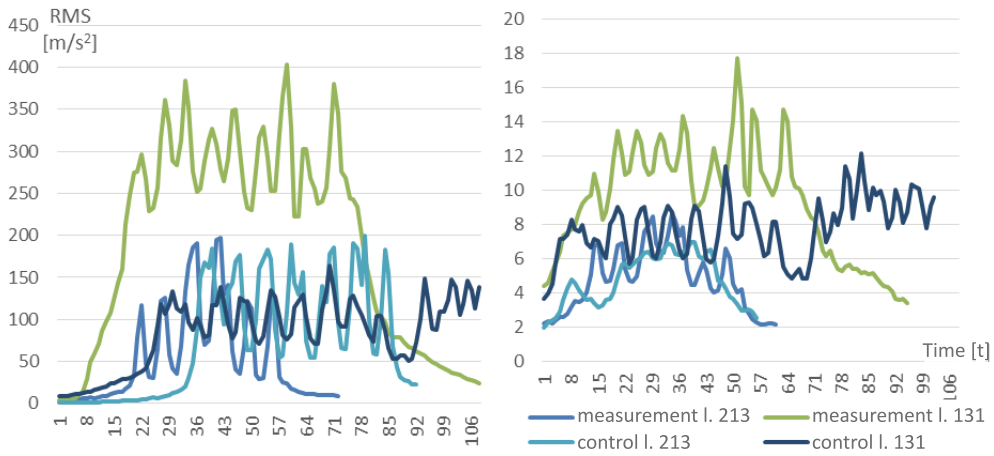

Fig. 5. Measurement results recorded by a single-axis sensor (left) and a three-axis sensor, direction X (right) for a track section with a squat defect – RMS acceleration values [authors' own work]

rail foot and by a three-axis sensor in direction X – according to the train movement direction.

The maximum values recorded by the single-axis sensor for the track section with a squat defect on line no. 131 amounted to 400 m/s^2. In the case of line no. 131, the values of acceleration of travel over the squat defect were four times higher than the values of signals recorded on the control track section. In the case of line no. 213, the recorded values were two times higher than those recorded on the control track section. The acceleration values recorded by the three-axis sensor for direction X were twenty times lower than the acceleration values recorded by the single-axis sensor. In the case of line no. 131, the maximum RMS value obtained for the three-axis sensor in direction X was 18 m/s^2, which is two times more than the values obtained for the control track.

Figure 6 presents measurement results provided by a three-axis sensor for direction Y – transverse to the rail-borne vehicle movement direction – and for direction Z – perpendicular to the rail-borne vehicle movement direction – for travel along a track section with a squat defect.

The RMS values of vibration acceleration for line 131 recorded during travel along a track section with a defect in axis Y were nine times higher than in the case of the control track section. The maximum value for axis Y was 98 m/s^2. The results given by the three-axis sensor in direction Z are ten times lower than those recorded by the single-axis sensor.

Figure 7 presents a comparison of the RMS values of vibration acceleration for the control track section with a track section featuring a spalling defect on lines no. 213 and no. 131.

When trains travelled along a section with a spalling defect, the single-axis sensor recorded values similar to those recorded on the control track section on line no. 213. In the case of the results recorded by the three-axis sensor in direction X, the RMS values obtained for travelling over the defect were two times higher than the values recorded on the control track for both railway lines.

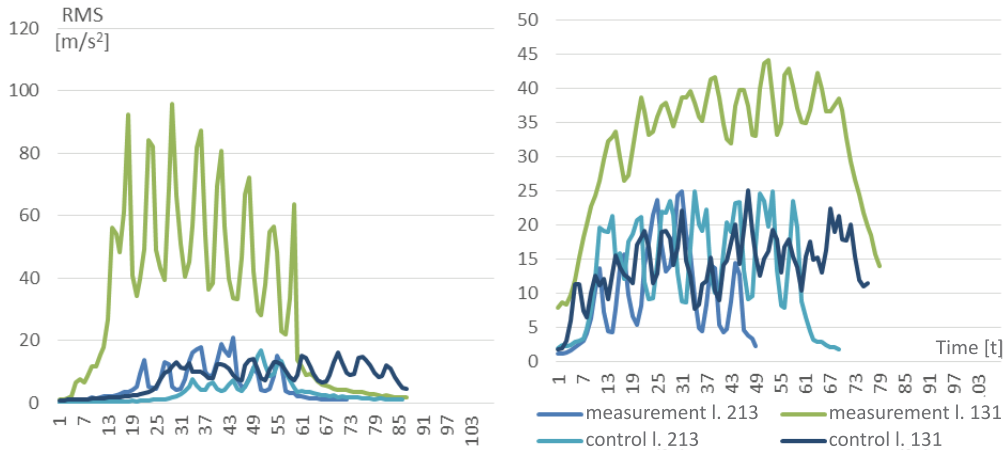

Fig. 6. Measurement results recorded by a three-axis sensor, direction Y (left) and direction Z (right) for a track section with a squat defect – RMS acceleration values [authors' own work]

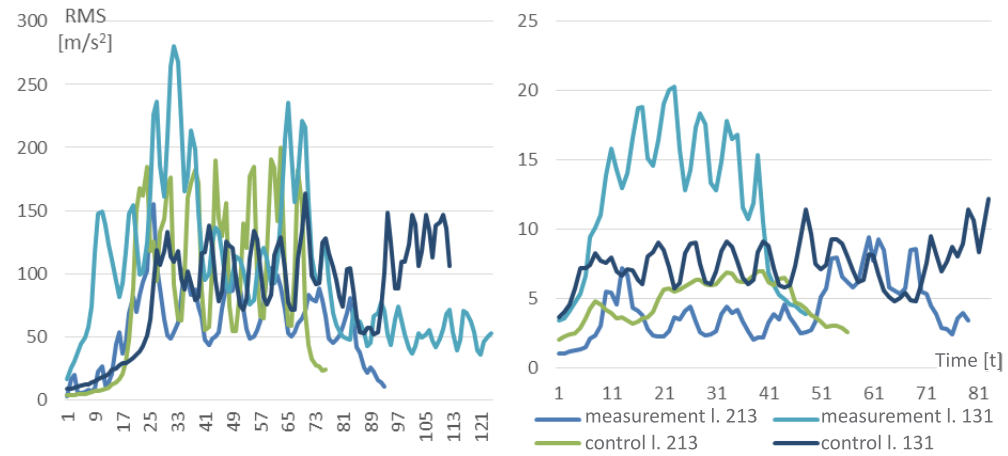

Fig. 7. Measurement results recorded by a single-axis sensor (left) and a three-axis sensor, direction X (right) for a track section with a spalling defect – RMS acceleration values [authors' own work]

Figure 8 presents measurement results provided by a three-axis sensor for direction Y and direction Z for travel over a track section with a spalling defect.

The maximum RMS value was recorded by the three-axis sensor in direction Y for the measurement on line no. 131, amounting to 32 m/s^2. In the case of both railway lines, the recorded values were two times higher than the values for the control track section in direction Y. The results of the measurements performed using the three-axis sensor in direction Z showed values for travelling over the defect that were two times lower than in the case of the values for the control track section.

Figure 9 shows a comparison of the RMS values of vibration acceleration for the single-axis sensor and the three-axis sensor in direction X for the control track section and the track section with a running surface defect no. 221 on lines 213 and 131.

The values of the results recorded by the single-axis sensor placed under the rail foot were similar to those recorded for travelling over the spalling defect. The three-axis sensor in direction X showed values which were two times higher for travelling over a defective track section than in the case of the control track section.

Figure 10 shows a comparison of the RMS values of vibration acceleration for the three-axis sensor in directions Y and Z for the control track section and the track section with a running surface defect no. 221 on lines 213 and 131.

The results obtained for travelling over a running surface defect, as recorded by the three-axis sensor in direction Y, featured values which were, on average, five times higher than in the case of values for the control track section on line no. 131. No similar relationship occurred on line no. 213. The measurements performed using the three-axis sensor for direction Z produced similar values for travelling over the defect and over the control track section in the case of both railway lines.

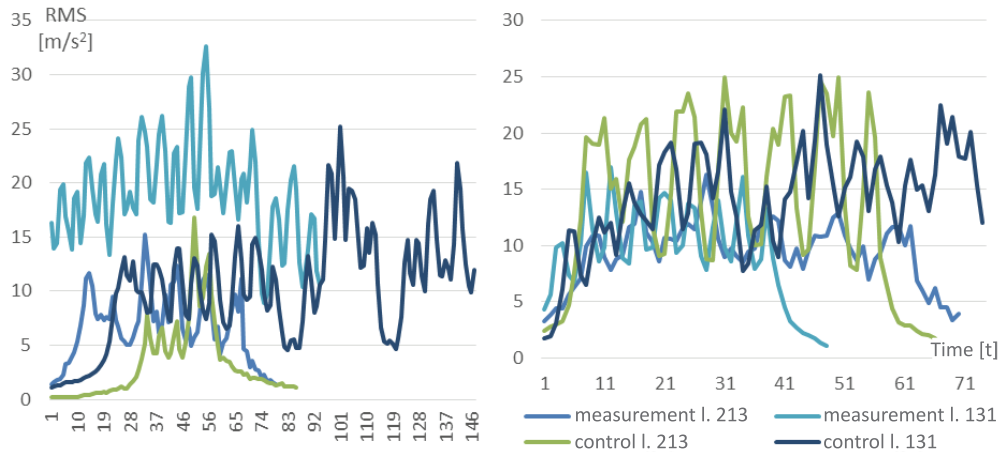

Fig. 8. Measurement results recorded by a three-axis sensor, direction Y (left) and direction Z (right) for a track section with a spalling defect – RMS acceleration values [authors' own work]

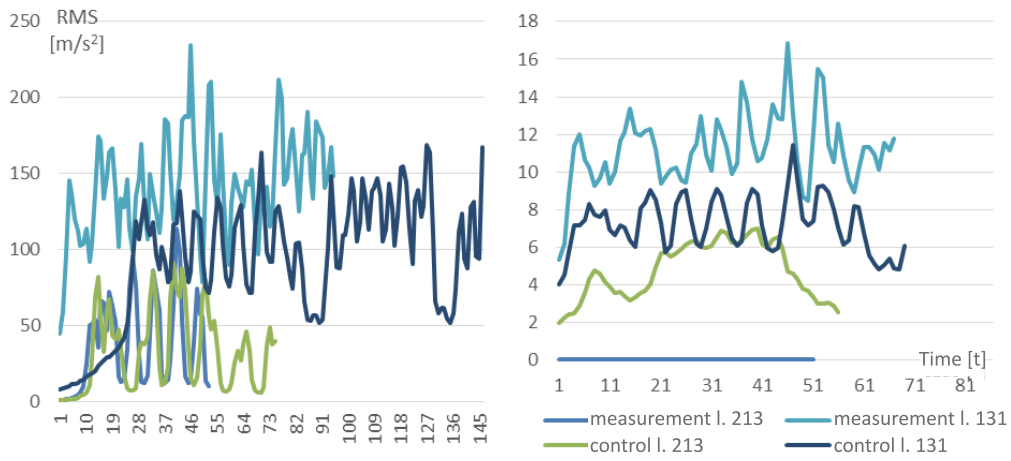

Fig. 9. Measurement results recorded by a single-axis sensor (left) and a three-axis sensor, direction X (right) for a track section with a running surface defect – RMS acceleration values [authors' own work]

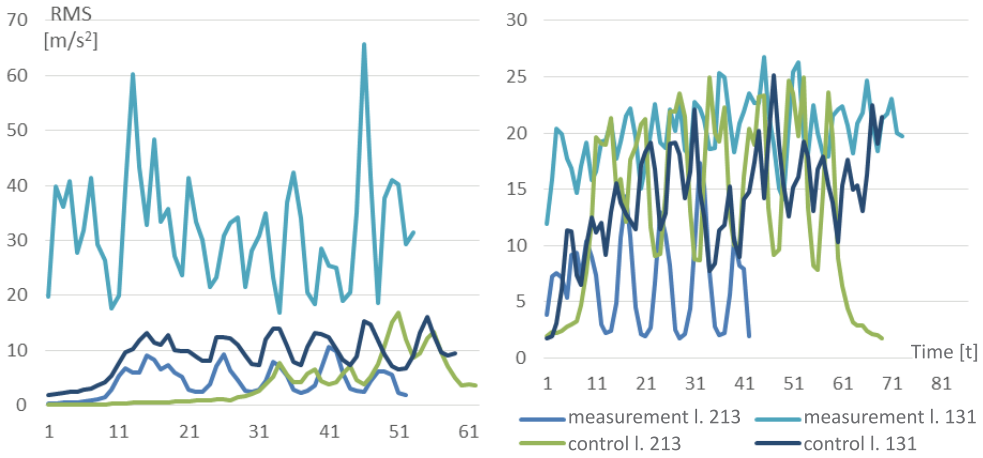

Fig. 10. Measurement results recorded by a three-axis sensor, direction Y (left) and direction Z (right) for a track section with a running surface defect – RMS acceleration values [authors' own work]

4. Conclusion

The article shows that the conducted tests prove that it is reasonable to pursue further analyses in order to determine the condition of the rail running surface and discusses an analysis of the possible ways to identify the occurring defects appearing during the utilisation of railway lines. It appears just as reasonable to explore the relationship between the defect types and the characteristics of the vibration signal.

During measurements, the 4513-B-001 vibration sensor was exposed to impacts beyond the measurement range, which has been considered in the compilation of the obtained results. Using a sensor with a broader dynamic range is recommended if measurements are to be continued.

The obtained results of vibration measurement performed at one measurement point offered a similar value distribution for particular vibration directions, regardless of the train speed or train set composition.

In the context of further tests, the authors plan to extend the base of measurement data by including additional railway lines with defect parametrisation and by taking tests performed on non-standard superstructures into consideration. In addition, the authors intend to continue their tests with an increased number of measurement points, including a seismic transducer that would enable the monitoring of vibration of the soil below the track superstructure.

Literature

1. Cempel C.: *Wibroakustyczna diagnostyka maszyn* [Vibroacoustic machine diagnostics], Wydawnictwa Naukowo-Techniczne PWN, Warszawa, 1989.
2. Kaewunruen S., Aikawa A., Remennikov A.: *Vibration attenuation at rail joints through under sleeper pads*, Procedia Engineering, 2017, nr 189, s. 193–198.
3. Katalog wad w szynach [Rail defects catalogue], PKP Polskie Linie Kolejowe S.A., Warszawa, 2005.
4. Li Z.: *Squats on railway rails*, in R. Lewis & U. Olofsson (Eds.), Wheel-rail interface handbook Cambridge, UK: Woodhead Publishing Limited, 2009, (pp. 409–436).
5. Licow R., Tomaszewski F., Urbaniak M.: *Badania wstępne możliwości oceny stanu powierzchni tocznej szyn za pomocą zjawisk wibroakustycznych* [Preliminary study into the possibility of assessment the rolling surface conditions of the raile using wibroacustic phenomena], Archiwum Instytutu Inżynierii Lądowej, tom 25, s. 255–265, 2017.
6. Pacyna J., Krawczyk J.: *Mechanizm powstawania uszkodzeń typu „squat" w szynach kolejowych* [Mechanism of "squat" type damage in railway rails], XIX Konferencja Naukowo-Techniczna Huty Katowice S.A., listopad 1999, Rogoźnik, s. 126–147.
7. Pacyna J., Krawczyk J.: *Mechanizm powstawania uszkodzeń typu „wybuksowanie" i „zużycie faliste" w szynach kolejowych* [Mechanism of "buckling" and "wavy wear" damage in railway rails], XIX Konferencja Naukowo-Techniczna Huty Katowice S.A., listopad 1999, Rogoźnik, s. 126–147.
8. Licow R., Tomaszewski F.: *Identyfikacja wad powierzchni tocznej szyn za pomocą sygnału wibroakustycznego* [Identifying Rail Running Surface Defects by Means of Vibroacoustic Signals], Problemy Kolejnictwa, 2019, z. 185, s. 71–76
9. www.bruel.com.